EPR Study of Cu^{2+} Doped Fast-Proton Conductor $K_3H(SO_4)_2$ in the Temperature Range 100–450 K

A. Ostrowski, W. Bednarski and S. Waplak

Institute of Molecular Physics, Polish Academy of Sciences
Smoluchowskiego 17, 60-179 Poznań, Poland

(Received July 31, 2003; revised version October 14, 2003)

The $K_3H(SO_4)_2$ doped with Cu^{2+} ion was studied in detail by X-band CW EPR. Two kinds of Cu^{2+} complexes (magnetically and structurally nonequivalent) denoted as Cu^{2+}(I) and Cu^{2+}(II) were found. Spin-Hamiltonian parameters, direction cosines, and coordination of Cu^{2+} ion were determined at room temperature. The superhyperfine structure was observed below 250 K as a result of interacting of Cu^{2+} ion with four equivalent protons ($I = 1/2$). Temperature studies of $K_3H(SO_4)_2$ crystal show that interbond motion as a precursor of superprotonic phase transition occurs at above ≈ 250 K.

PACS numbers: 61.50.–f, 76.30.–v

1. Introduction

The transport of protons in hydrogen-bonded system is a long standing problem that has not yet been satisfactorily explained.

The properties of the proton potential and the proton–proton interaction lead to possible coherence in proton motion with the concept of topological solitons [1]. On the other hand, the propagation of solitons in nonlinear lattice with an impurity has been extensively studied theoretically [2, 3]. To perform such systematic experimental studies it is necessary to use several types of impurities with well defined concentrations and site position.

The aim of this work are studies of coordination and spin-Hamiltonian parameters of Cu^{2+} ($3d^9$) paramagnetic ion in $K_3H(SO_4)_2$ (KHS) crystal which be-

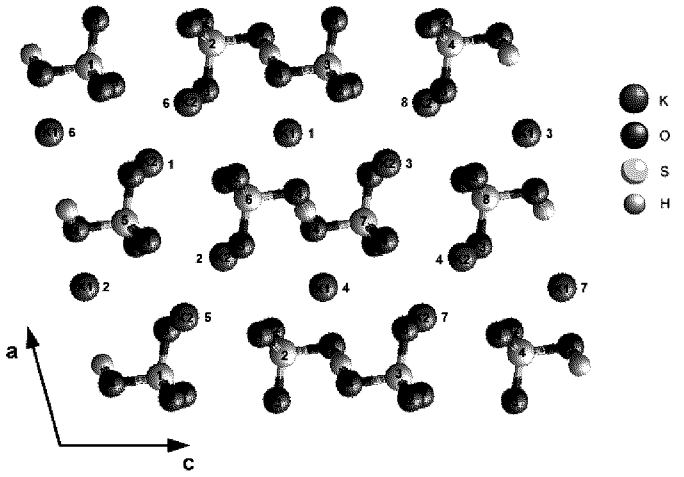

Fig. 1. The view of $K_3H(SO_4)_2$ structure along the b axis.

longs to $M_3H(SO_4)_2$ family of hydrogen-bonded insulators, where M = K, Cs, Rb, NH_4 [4, 5].

The KHS crystal has specific crystal structure which contains a "zero-dimensional" hydrogen-bond network consisting of isolated $SO_4^{2-}-H\ldots SO_4^{2-}$ dimers. The K^+ ions occupy two different sites: K1 symmetric site on twofold axis (parallel to the b axis) and K2 sites related by screw axis (Fig. 1). X-ray data [5] show that KHS at room temperature (RT) belongs to the space group $A2/a$, $Z = 4$ with $a = 9.777$ Å, $b = 5.674$ Å, $c = 14.667$ Å and $\beta = 102.92°$ lattice parameters. Below 471 K, KHS exhibits ferroelastic properties and above 471 K reveals high proton conductivity order $10^{-1}\ \Omega^{-1}\ \mathrm{cm}^{-1}$ [6]. In superprotonic (paraelastic) phase the atoms slightly displace to more symmetric position resulting in crystal structure symmetrization with the space group $R\bar{3}m$.

2. Crystal growth

Hexagonal plate-like $K_3H(SO_4)_2$ crystals were grown isothermally at 300 K from the saturated aqueous solution containing 19 wt% K_2SO_4, 12.7 wt% H_2SO_4 and 1 wt% $CuSO_4{\cdot}5H_2O$. Optical investigation of the single crystal in polarized light reveals the ferroelastic $n \times 60°$ domain pattern. EPR studies were carried out on a single-domain sample cut off under the polarization microscope. The Cu^{2+} ion concentration in crystal under study was of order of 300 ppm.

3. EPR spectra anisotropy and spin-Hamiltonian parameters at RT

The XYZ orthogonal laboratory frame chosen for the EPR anisotropy pattern was related to the $\boldsymbol{a}$, $\boldsymbol{b}$, and $\boldsymbol{c}$ crystallographic axes as follows: $\boldsymbol{X} \parallel \boldsymbol{a}$, $\boldsymbol{Y} \parallel \boldsymbol{b}$, and $\boldsymbol{Z} \parallel \boldsymbol{a} \times \boldsymbol{b}$.

Figure 2 shows the EPR spectrum with magnetic field $\boldsymbol{B}$ parallel to the X axis (a) and Y axis (b). In Fig. 3 the EPR line angular dependence is shown.

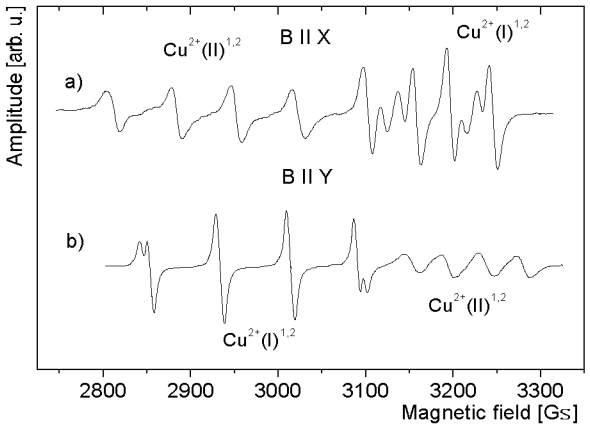

Fig. 2. EPR spectra of the single-domain $K_3H(SO_4)_2$:Cu^{2+} crystal at room temperature. The external magnetic field $\boldsymbol{B}$ is parallel to the X axis (a) and Y axis (b), respectively.

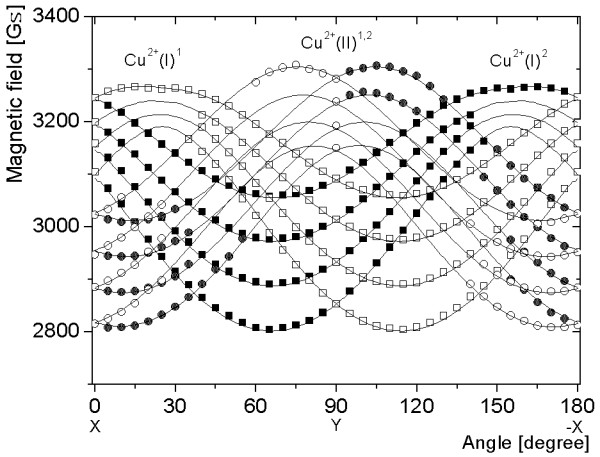

Fig. 3. The simplified angular dependence of the resonance fields for Cu^{2+} complexes in the XY plane which include only $\boldsymbol{g}$, $\boldsymbol{A}$, and $\boldsymbol{P}$ for the ^{63}Cu isotope. The forbidden transition lines are omitted. The symbols represent the experimental data for Cu^{2+}(I) (squares) and Cu^{2+}(II) (circles) complexes. The solid lines were calculated using Eq. (1) and parameters collected in Table.

There are two types of magnetically non-equivalent complexes denoted as Cu^{2+}(I) and Cu^{2+}(II). Due to the point symmetry $2/m$ in the single-domain crys-

TABLE

Spin-Hamiltonian parameters and direction cosines of the $Cu^{2+}(I)^{1,2}$ and $Cu^{2+}(II)^{1,2}$ complexes in $K_3H(SO_4)_2$:Cu^{2+} at room temperature for ^{63}Cu isotope.

Complex	Principal g-values	Principal A-values in [Gs]	Principal P-values in [Gs]	Direction cosines of the principal direction of g and A tensors		
				X	Y	Z
$Cu^{2+}(I)^{1,2}$	2.066(5)	24(2)	$P = 6(1)$	0.935	0.101	$\mp$0.340
	2.093(5)	6(2)	$Q < 1$	$\pm$0.156	$\pm$0.743	0.650
	2.435(5)	101(2)		–0.318	0.661	$\mp$0.679
$Cu^{2+}(II)^{1,2}$	2.105(8)	30(2)		0.615	0.252	$\pm$0.747
	2.065(8)	54(2)		$\mp$0.257	$\pm$0.960	–0.112
	2.445(8)	80(2)		0.746	0.123	$\pm$0.655

tal there are two structurally nonequivalent sites $Cu^{2+}(I)^1$ and $Cu^{2+}(I)^2$ for I-type complex and two $Cu^{2+}(II)^1$ and $Cu^{2+}(II)^2$ for II-type complex (see Fig. 2, Fig. 3, and Table).

The EPR lines of each complex consist of four hyperfine structure lines resulting from interaction of the electron spin $S = 1/2$ of the Cu^{2+} ion and its nuclear spin $I = 3/2$.

The integral intensity of the single component of the I-type complex is approximately 2.5 times larger than II-type complex. The outer lines of the I-type complex in Fig. 2 are split as a result of the appearance of two copper isotopes $^{63}Cu/^{65}Cu$. The similar effect is observed for II-type complex.

Due to non-zero value of quadruple interaction tensor $\boldsymbol{P}$, the distances between four hyperfine structure lines are not equidistant and the forbidden transition structure lines ($\Delta M_s = \pm 1$, $\Delta m = \pm 1$) occurs around perpendicular g-tensor orientation (see Fig. 2a).

The EPR spectrum of Cu^{2+} centre is described by the spin-Hamiltonian

$$H = \beta \boldsymbol{B} \boldsymbol{g} \hat{S} + \hat{S} \boldsymbol{A} \hat{I} + \hat{I} \boldsymbol{P} \hat{I}, \tag{1}$$

where $\boldsymbol{g}$ is the spectroscopic tensor, $\boldsymbol{A}$ is the hyperfine tensor, $\boldsymbol{P}$ is the quadrupole tensor, $\hat{S}$ and $\hat{I}$ are the Cu^{2+} electronic and nuclear spin operators, respectively.

For both complexes the principal values of the $\boldsymbol{g}$ and $\boldsymbol{A}$ tensors as well as direction cosines of the main directions were found from the angular dependence of the lines, and from hyperfine splitting in the three mutually perpendicular planes XY, ZY, ZX.

The proper formulae for resonance fields along principal $\boldsymbol{g}$ and $\boldsymbol{A}$ tensor direction in the case of rhombic symmetry for Cu^{2+} ion and for allowed transition ($\Delta M_s = \pm 1$, $\Delta m = 0$) were given by Sakaguchi et al. [7]. In order to obtain principal values of $\boldsymbol{g}$, $\boldsymbol{P}$, and $\boldsymbol{A}$ tensors we have measured the positions of hyperfine structure resonance lines in the principal directions x, y, z, and used the modified [7] equations

for $B \parallel z$,

$$B_m^z = B_{0z} - mA_z - \frac{1}{4}\left(\frac{15}{4} - m^2\right)\frac{g_x^2A_x^2 + g_y^2A_y^2}{g_z^2B_m^z}$$
$$-4\frac{m}{2}\left(\frac{15}{2} - 2m^2 - 1\right)\frac{\frac{1}{36}[P(g_y - g_x) + 3Q(g_x + g_y)]^2}{g_z^2A_z},$$

for $B \parallel y$,

$$B_m^y = B_{0y} - mA_y - \frac{1}{4}\left(\frac{15}{4} - m^2\right)\frac{g_x^2A_x^2 + g_z^2A_z^2}{g_y^2B_m^y}$$
$$-\frac{m}{2}\left(\frac{15}{2} - 2m^2 - 1\right)\frac{\{Pg_z - \frac{1}{6}[P(g_y - g_x) + 3Q(g_y + g_x)]\}^2}{g_y^2A_y},$$

for $B \parallel x$,

$$B_m^x = B_{0x} - mA_x - \frac{1}{4}\left(\frac{15}{4} - m^2\right)\frac{g_y^2A_y^2 + g_z^2A_z^2}{g_x^2B_m^x}$$
$$-\frac{m}{2}\left(\frac{15}{2} - 2m^2 - 1\right)\frac{\{Pg_z + \frac{1}{6}[P(g_y - g_x) + 3Q(g_y + g_x)]\}^2}{g_x^2A_x}, \qquad (2)$$

where $B_{0i} = h\nu/g_i\beta$ $(i = x,\ y,\ z)$; $P = \frac{3}{2}P_z$ and $Q = \frac{1}{2}(P_x - P_y)$ are the components of tensor $\boldsymbol{P}$, m is the magnetic nuclear quantum number.

4. Coordination of Cu^{2+} ion in $K_3H(SO_4)_2$

The coordination of the Cu^{2+} ion in crystal lattice can be determined from the X-ray studies, superhyperfine structure of the EPR lines of Cu^{2+} ion, direction cosines of the main crystal field directions x, y, z as well as from the relations between components of the $\boldsymbol{g}$ and $\boldsymbol{A}$ tensors.

In the case of copper complex of low symmetry the ground state is mixed (i.e. wave function of the ground state is a linear combination of the ground and excited states). If the following relations between spin-Hamiltonian parameters hold:

$$g_z > g_y > g_x \quad \text{or} \quad g_z > g_x > g_y, \quad |A_z| > |A_x|, \quad |A_z| > |A_y|, \qquad (3)$$

then the coordination of Cu^{2+} ion has orthorombic symmetry like in our case (Table). The z-axis direction of Cu^{2+} complex is nearly parallel to the normal of the main coordination plane.

The position of the admixture ion in crystalline lattice should be also considered from the point of view of the local charge compensation of the admixed ions.

We performed detailed analysis of possible positions of Cu^{2+} ion in the crystal lattice: (a) the vacancy left over by K1 ion (Fig. 4a); (b) an interstitial position

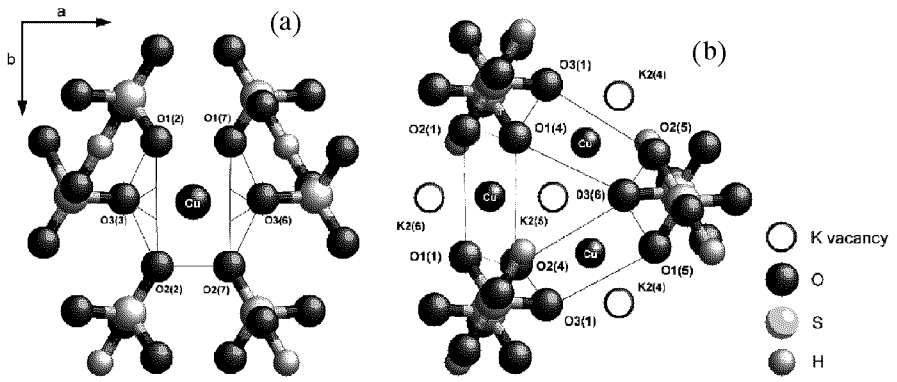

Fig. 4. The neighbourhoods of Cu^{2+} ion in monoclinic phase: (a) replacing a K1 ion, (b) occupying an interstitial position between vacancies of K2 ions. The possible coordination planes were marked as white quadrangle for I-type and grey for II-types complexes, respectively.

between two vacancies of nearest-neighbouring K2 (Fig. 4b). In both cases nearest oxygen atoms of neighbouring SO_4 groups form quadrangles which coordinate Cu^{2+} ion.

For I-type complex it is possible to find a coordination plane determined by four oxygen atoms with the angles 18° and 20° between the normal and the z-axis, respectively. One can find the similar relation II-type complex with the angles 17° (see Fig. 4). for Unfortunately, the choice of the position of Cu^{2+} ion

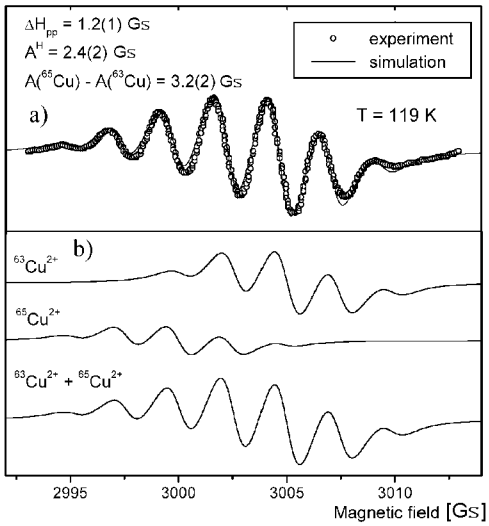

Fig. 5. (a) The experimental (circles) and simulated (lines) superhyperfine spectrum for Cu^{2+} in the $K_3H(SO_4)_2$ at 119 K. (b) Simulated isotopic components and total spectrum for transition: $(M_s = 1/2,\ m = 3/2) \leftrightarrow (M_s = -1/2,\ m = 3/2)$.

is still not unique. Fortunately, below 250 K the EPR superhyperfine structure (SHFS) appears. Detailed analysis of the line position and line width of transition $(M_s = 1/2, m = 3/2) \rightarrow (M_s = -1/2, m = 3/2)$ shows that Cu^{2+} ion interacts with four equivalent protons ($I = 1/2$). Figure 5 shows the experimental and simulated spectra. The spectrum consists of line of ^{63}Cu and ^{65}Cu isotopes and we assumed that the intensity ratio corresponds to the ratio of abundance of $^{63}Cu/^{65}Cu$ which is equal to 2.24. The difference of hyperfine constants for the isotopes ^{63}Cu and ^{65}Cu is equal to 3.2(2) Gs, the superhyperfine interaction constant is $A^H = 2.4(2)$ Gs and line width $\Delta H_{pp} = 1.2(1)$ Gs.

The presence of SHFS indicates that Cu^{2+} ion occupies interstitial position between vacancies of K2 ions (see Fig. 4b), because only in this position an interaction of Cu^{2+} with four protons in $SO_4^{2-} - H \ldots SO_4^{2-}$ dimers is possible.

The foregoing results and values of direction cosines show that case (b) is correct and coordination surrounding of Cu^{2+} ion consists of oxygen atoms denoted as O1(4), O3(1), O2(5), O3(6) for I-type complex (white quadrangle) and O2(1), O1(4), O2(4), O1(1) (grey quadrangle) for II-type of complex.

5. EPR spectra evolution versus temperature

KHS crystal was studied in temperature range 100–450 K. Observation of EPR spectra at higher temperatures is hardly possible because of the line width broadening.

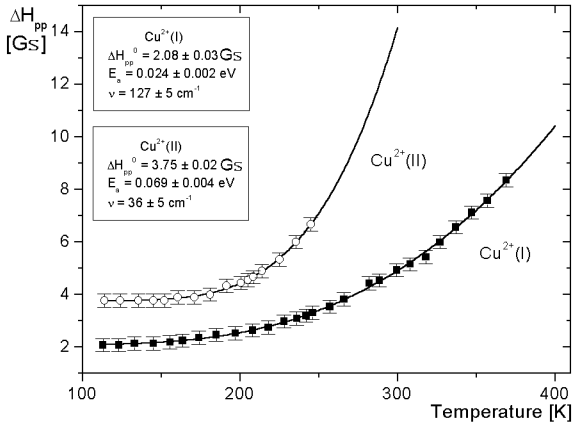

Fig. 6. Temperature dependence of ΔH_{pp} for two types of Cu^{2+} complexes.

Figure 6 presents $\Delta H_{pp}(T)$ for transition $(M_s = 1/2,\ m = 3/2) \leftrightarrow (M_s = -1/2,\ m = 3/2)$, which is well described by modified equation [8]:

$$\Delta H_{pp} = \Delta H_{pp}^0 \left[1 + e^{-\delta/2kT} \operatorname{cth}^2 \left(\frac{h\nu}{2kT}\right) e^{-E_a/kT}\right], \tag{4}$$

where h is the Planck constant, k is the Boltzmann constant, δ is the orbital splitting in the tetragonal crystal field, E_a is the activation energy and ν is the frequency of lattice mode.

Equation (4) has been introduced by Altshuler and Walijev [9] for successful EPR line width description in solid electrolyte. The basic idea of Eq. (4) is that for the time longer than correlation time of "spin–lattice interaction" paramagnetic cluster of MX_6 type can be characterized by set of normal coordinate Q_i. This model called as "ionic liquid" is also used to line width description in superionic conductors [10].

The Raman spectra have been measured in KHS by Damak et al. [11]. They have found that nine sharp lines in the frequency region of 173–39 cm^{-1} respond to the lattice modes. They are shared in vibration and translation movements of SO_4^{2-} and K^+ ions. The fact that Cu^{2+} line widths in KHS are well described by Eq. (4) with the values of lattice mode frequencies 127 cm^{-1} and 36 cm^{-1} allow us to conclude that far below transition to superionic phase Cu^{2+} complexes in KHS behave as "ionic liquid cage".

The g_z component of spectroscopic $\boldsymbol{g}$-tensor of Cu^{2+} complexes have the averaged values at about 400 K, i.e. $\approx$ 70 K below superionic phase transition (Fig. 7a). The direction cosines of g_z and K2 vacancies which compensate an excess charge of Cu^{2+} ions are parallel. At low temperature (below 400 K) two distinct g_z values of Cu^{2+}(I) and Cu^{2+}(II) complexes mean that there are two nonequivalent K2 (vacancy) positions in the crystal lattice. At about 400 K there is only one (averaged) K2 position. This statement collaborates with Rb^{87} NMR data [12] in isomorphous $Rb_3H(SO_4)_2$ crystal of $Me_3H(SO_4)_2$ family, where about 50 K below T_c only one Rb^+ ion was observed instead of three at RT. This averaging process is not valid for two other g_x and g_y components which describe a different deformation of Cu(I) and Cu(II) coordination planes.

The hyperfine interaction constant A_z linearly decreases with temperature increasing for both types of complexes (Fig. 7b). The temperature dependence of $A(T)$ for powder KHS:Cu^{2+} showed that $\partial A_z/\partial T$, $\partial A_x/\partial T$, and $\partial A_y/\partial T$ are equal to –0.043, 0.033 and –0.060 Gs K^{-1}, respectively. Cu^{2+} in KHS bonds four $SO_4{-}H\ldots SO_4$ dimers. The dynamics of Cu^{2+} complexes is predominantly determined by the thermally induced SO_4 vibration and proton movement as well. Two types of proton movements i.e. "intrabond" and "interbond" are distinguished in fast proton conductor [12, 13].

Additionally, we have observed SHFS resonance lines at temperatures below 250 K (Fig. 8) and SHFS constant A^H does not change below this temperature within experimental error. Superhyperfine structure in EPR spectra of Cu^{2+} ion is due to electron spin ($S = 1/2$) interaction with four equivalent protons on Cu–O–S...H path. The temperature speeds both intra and interbond motions. The "vanishing out" of the superhyperfine structure versus temperature may be evoked by individual line broadening or by dynamic line width effects. In the case

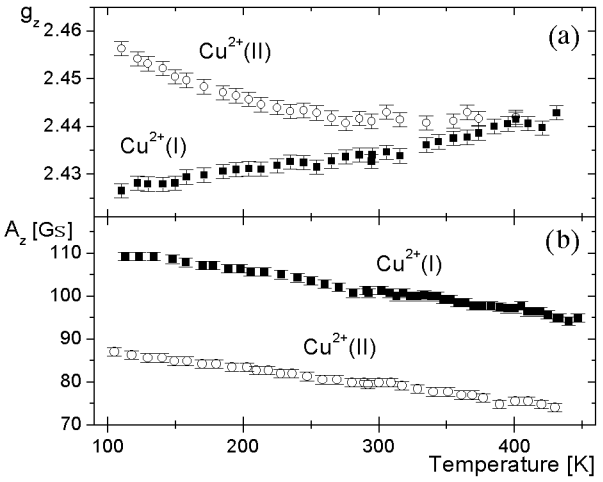

Fig. 7. Temperature dependence of g_z (a) and A_z (b) for two types of Cu^{2+} complexes.

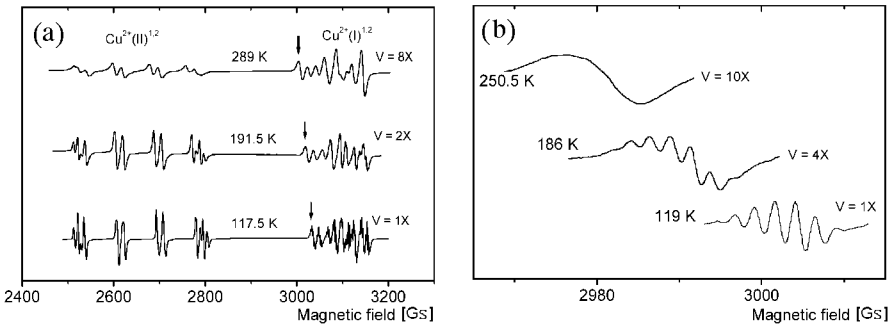

Fig. 8. Evolution of the superhyperfine structure versus temperature: (a) full spectra, (b) one SHF component indicated on the left part by arrows.

of line width broadening the spectrum consisting of five (SHF) components should have almost the same intensity in the temperature range where the Boltzmann law is flat enough. By comparison of spectra at 119 and 186 K we can see only about 10% line width broadening. Such broadening should lead to the line amplitude change of about 20% ($I \approx A(\Delta H_{\rm pp})^2$; here A is the amplitude, $\Delta H_{\rm pp}$ is the line width). In reality the line intensity lowering is of order of hundreds %. It is the evidence that amount of nuclear (hydrogen) spins do not participate in static spectra. Instead they give an "averaged" broad line in the centre of SHF spectrum. Similarly as it was observed by Evora and Jaccarino [10] such SHFS "vanishing out" appears for $\tau_{\rm c}{}^{-1} \geq A^{\rm H}/\hbar = 4 \times 10^7$ Hz (in our case), where $\tau_{\rm c}$ is the proton jump time and $A^{\rm H}$ is the SHF constant. Only the last model leads to reasonable data of computer simulation.

6. Conclusions

We have determined unambiguously the site positions of Cu^{2+} complexes in KHS lattice. Our data show that even far below 471 K the KHS lattice is "soft". Two non-equivalent K2 site positions at RT are averaged to one at about 400 K (g_z equivalency). Because four $SO_4^{2-}-H\ldots SO_4^{2-}$ are bonded by Cu^{2+} ion we can conclude on the basis on lack of g_x, g_y and $\boldsymbol{A}$ tensors averaging that the dimer-like structure is preserved up to phase transition temperature. The influence of the lattice dynamics on the line width is well described by Eq. (4) usually applied to solid electrolyte. It is our statement that in KHS "vanishing out" of superhyperfine proton structure in Cu^{2+} spectra appears at temperature when proton hopping intrabond rate $\tau_c^{-1} \geq 4 \times 10^7$ Hz.

Acknowledgment

This work was supported by the State Committee for Scientific Research grant 5PO3B06120.

References

[1] V.Ya. Antonchenko, A.S. Davydov, A.V. Zolotaryuk, *Phys. Status Solidi B* **115,** 631 (1983).

[2] S. Yomosa, *J. Phys. Soc. Jpn.* **51,** 3318 (1982).

[3] Quiming Li, St. Pnevmakitos, E.N. Economou, C.M. Soukoulis, *Phys. Rev. B* **37,** 3534 (1988).

[4] A.I. Baranov, V.P. Kniznichenko, L.A. Shuvalov, *Ferroelectrics* **100,** 135 (1989).

[5] Y. Noda, S. Uchiyama, K. Kafuku, H. Kasatani, H. Terauchi, *J. Phys. Soc. Jpn.* **59,** 2804 (1990).

[6] R.H. Chen, R.Y. Chang, C.S. Shern, T. Fukami, *J. Phys. Chem. Solids* **64,** 553 (2003).

[7] V. Sakaguchi, Y. Arata, S. Fujiwara, *J. Magn. Reson.* **9,** 118 (1973).

[8] S.A. Altshuler, B.M. Kozyrev, *Electron Paramagnetic Resonance*, Nauka, Moskva 1972 (in Russian).

[9] S.A. Altshuler, K.A. Walijev, *Zh. Eksp. Teor. Fiz.* **35,** 947 (1958).

[10] C. Evora, V. Jaccarino, *Phys. Rev. Lett.* **24,** 1557 (1977).

[11] M. Damak, M. Kamoun, A. Daoud, F. Romain, A. Lautie, A. Novak, *J. Mol. Struct.* **130,** 245 (1985).

[12] J. Dolinšek, U. Mikac, J.E. Javoršek, G. Lahajnar, R. Blinc, *Phys. Rev. B* **58,** 8445 (1998).

[13] V.H. Smidth, E. Uehling, *Phys. Rev.* **126,** 447 (1962).